An optimized BP neural network based on genetic algorithm for static decoupling of a six-axis force/torque sensor

Liyue Fu[1] and Aiguo Song[1,2]

1 School of Instrument Science and Engineering, Southeast University, Nan Jing, China
E-mail: a.g.song@seu.edu.cn

Abstract. In order to improve the measurement precision of 6-axis force/torque sensor for robot, BP decoupling algorithm optimized by GA (GA-BP algorithm) is proposed in this paper. The weights and thresholds of a BP neural network with 6-10-6 topology are optimized by GA to develop decouple a six-axis force/torque sensor. By comparison with other traditional decoupling algorithm, calculating the pseudo-inverse matrix of calibration and classical BP algorithm, the decoupling results validate the good decoupling performance of GA-BP algorithm and the coupling errors are reduced.

1. Introduction

For ideal six-axis force/torque sensors, each output value depends only on the force/torque loaded in this direction and not in the other five directions. But actually, for the reason of the mechanical structure of elastic body, the precision of machine operation, strain gauges bonding technology, and measurement methods, etc. almost every force/moment component exerted on sensor impacts on all the output signals, dimensional coupling. Only when dimensional coupling interference is solved, accurate measurement can be achieved.

Dimensional coupling elimination is a key issue for six-axis force/torque sensors. A variety of decoupling algorithms are used to reduce or eliminate the coupling errors. In general, there are two decoupling methods of multi-dimensional force/torque sensors. One method is hardware decoupling, say, the design of 6-axis fore/torque sensors based on mechanism decoupling of the elastic body. Float beam structure [1] and sliding structure [2] are representative mechanical decoupling forms. The other method is software decoupling, decoupling algorithms. Calculating the pseudo-inverse matrix of calibration based on the Least Square Method (LSM) [3] is the most common decoupling algorithm. Due to the relationship between the input and output data of different tunnels is not always linear, Artificial Neural Network is widely used in decoupling algorithms of multi-dimensional force/torque sensors instead of the former method [4]. BP neural network is one of the most common neural networks used for decoupling algorithm [5] [6]. As a result of its local minimum, the decoupling accuracy of BP neural network is barely satisfactory.

With the rapid development of intelligent optimization algorithm, Genetic Algorithm (GA) is widely used in various areas, such as machine learning, pattern identification, control system optimization, and so forth. Aim at overcoming demerits of BP neural network, GA is introduced to optimize the decoupling network in this article.

As a method of seeking the optimum solution by simulating the natural evolution process, GA experts in searching large-scale, non-differentiable, multi-mode space and the gradient information. By doing selection, crossover, mutation and other genetic operations, a new population can be produced. As one

of the study hotspots in the intelligent computing, optimized BP neural network based on GA has been widely used in many fields [7][8][9]. Sun wei obtained the index values of the financial security of China's power industry in 2011 according to the tested prediction model based on BP-GA algorithm [10]. Sharon Mano J. Pappu recommended ANN coupled GA to be employed for optimization of fermentative process due to its high accuracy and low prediction error [11]. Jia Weikuan [12] proposed the PLS-GA-RBF algorithm for classification of small sample. Above researchers have achieved good results, but they do not have a systematic description of the BP-GA decoupling model of 6-axis force/torque sensor. Consequently, One decoupling algorithm, optimized BP neural network based on Genetic Algorithm, is proposed in this paper.

2. Six-axis force/torque sensor and static calibration experiment

2.1. Mechanical structure

The mechanical structure of the 6-axis force/torque sensor consists of five parts: bottom cover, pedestal, elastic body, top cover and calibration pillar. The assembled structure of the sensor is shown in Figure 1(a). The performance of the sensor mainly relies on the mechanical structure of the elastic body. As shown in Figure 1(b), the structure of the elastic body is classical cross-beam structure, which is composed of cross beam, compliant beams, a central platform and flange.

(a) (b)

Figure 1. Prototype of the 6-axis force/torque sensor.

2.2 Calibration experiment

The experiment platform of the calibration tests is illustrated in Figure 2(a). A six-axis force/torque sensor can be fixed to the rotatable indexing plate to guarantee directions of loading forces or torques. Applying a torque in *x*/*y* direction M_x/M_y is shown in Figure 2(b), and Figure 2(c) shows calibration of F_z.

Generally, one force component is applied to the sensor on the condition that other forces/torques are set to zero in the static calibration experiment. However, neural network for decoupling of the six-axis force/torque sensor requires training samples to be more diversified, so as to make training samples provide more information. It is inadequate to carry out calibration test according to the foregoing, and the calibration method adopted in the paper is as follows.

Firstly, the traditional calibration experiments mentioned above are implemented. Secondly, according to the results of the calibration tests, we can roughly get the components with severe coupling interference. Thirdly, do further calibration tests. Exert force/torque on multiple axes with severe coupling interference simultaneously, and record output voltage of each axis. Thus, the calibration data is more diverse, which is very helpful to improve the decoupling accuracy of neural network. The calibration data obtained by applying F_x, in the case of $M_y=0, 0.5\ N \cdot m$ respectively, are totally 84 sets of data. Consequently, 504 sets of data were measured in 6 dimensions.

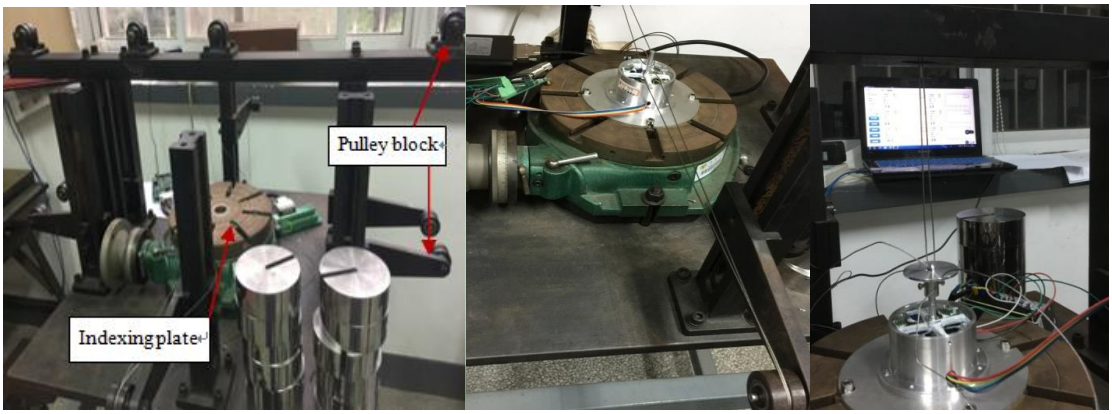

(a) (b) (c)

Figure 2. The calibration experiments setup.

3. Decoupling algorithms and results comparison

Calibration data is fed into the nonlinear decoupling model for decoupling calculation after data preprocessing such as removal of gross errors, systematic error correction, etc. and then the relationships between the input and output signals of the six-axis force/torque sensor are obtained. Two traditional decoupling algorithms are first simply introduced, then GA-BP algorithm is put forward, and their decoupling errors are compared in this section.

3.1. Decoupling algorithm based on calculating the pseudo-inverse matrix of calibration

The output value is proportional to the force or torque exerted in this direction. It can be assumed before analysis that the relationship between the output voltage and the force/torque in other direction is also linear. According to the static calibration experiment data, the input-output relationship can be expressed as shown in equation (1) after ignoring small elements below the order of 10^{-2} in the coefficient matrix.

$$\begin{bmatrix} U_{Fx} \\ U_{Fy} \\ U_{Fz} \\ U_{Mx} \\ U_{My} \\ U_{Mz} \end{bmatrix} = \begin{bmatrix} 1 & 0 & 0 & 0 & 0 & 0 \\ 0 & 1 & 0 & 0 & 0 & 0 \\ 0 & 0 & -1 & 0 & 0 & 0 \\ 0 & 1.732 & -1.34 & 1 & 0 & 0 \\ 0.914 & 0 & 0 & 0 & 1 & 0 \\ -0.239 & -0.137 & 0 & 0 & 0 & 1 \end{bmatrix} \begin{bmatrix} F_x \\ F_y \\ F_z \\ M_x \\ M_y \\ M_z \end{bmatrix} \tag{1}$$

Then, pseudo-inverse matrix of coefficient matrix is worked out, and equation (2) is as follows.

$$\begin{bmatrix} F_x \\ F_y \\ F_z \\ M_x \\ M_y \\ M_z \end{bmatrix} = \begin{bmatrix} 3.2082 & 0 & 0 & 0 & 0 & 0 \\ 0 & 3.0874 & 0 & 0 & 0 & 0 \\ 0 & 0 & -5.0302 & 0 & 0 & 0 \\ 0 & -5.3478 & -6.737 & 4.4643 & 0 & 0 \\ -5.6201 & 0 & 0 & 0 & 4.1859 & 0 \\ 0.7657 & 0.4243 & 0 & 0 & 0 & 2.021 \end{bmatrix} \begin{bmatrix} U_{Fx} \\ U_{Fy} \\ U_{Fz} \\ U_{Mx} \\ U_{My} \\ U_{Mz} \end{bmatrix} \tag{2}$$

Table 1. Decoupling precision of six dimensions.

Coupling error(FS%)	Fx	Fy	Fz	Mx	My	Mz
Type Ⅰ	0.22	0.3	0.36	0.48	0.83	0.56
Type Ⅱ	7.9	8.7	3.8	6.5	7.6	2.8

As can be seen from the equation (2), there is severe dimension coupling relationship between F_x and U_{My}, F_y and U_{Mx}, F_z and U_{Mx}, and so on. Decoupling precision of six dimensions which is calculated from Equation (2) is listed in Table 1. It can be concluded from Table 1that the maximum coupling error of type Ⅰ and type Ⅱ is 0.83% and 8.7%, respectively. The concepts of type Ⅰ and type Ⅱ error are illustrated in appendix section.

3.2. Decoupling algorithm based on BP neural network

The BP neural network is a kind of multilayer feed-forward network based on an error back-propagation algorithm for training. In this paper, architecture of the decoupling BP neural network is 6-10-6, as shown in Figure 3.

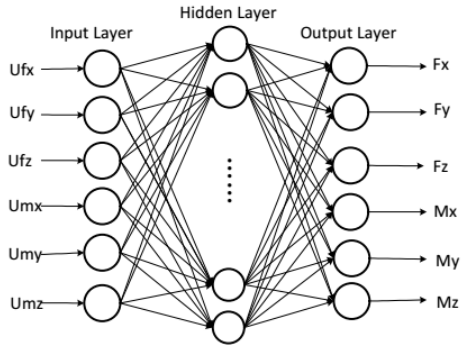

Figure 3. Architecture of the BP-NN model for decoupling.

Table 2. Decoupling precision of BP algorithm in six dimensions.

Coupling error(FS%)	Fx	Fy	Fz	Mx	My	Mz
Type Ⅰ	0.1	0.23	0.34	0.51	0.46	0.12
Type Ⅱ	2.4	2.3	2.5	1.8	2.9	1.4

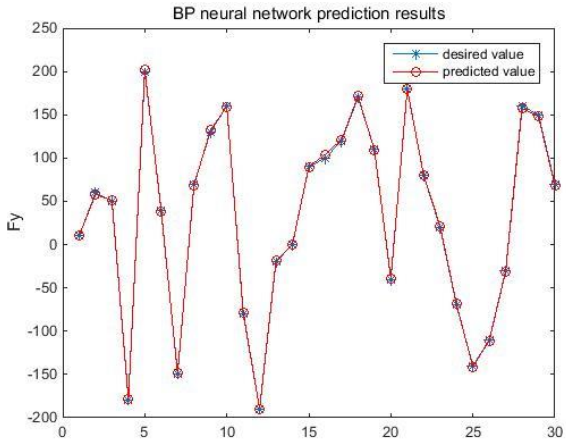

Figure 4. BP neural network prediction results of Fy.

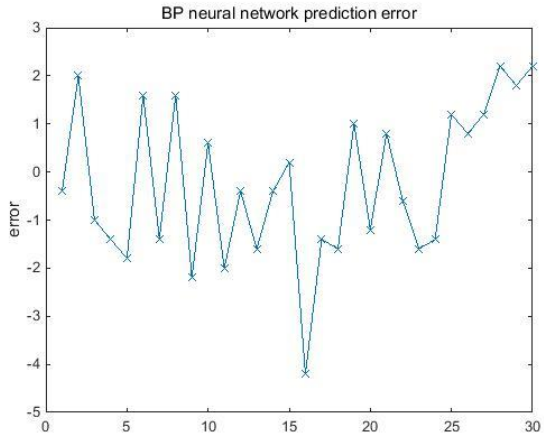

Figure 5. BP neural network prediction error.

A total of 500 sets of data are collected in calibration experiments. 450 of them were used as training samples and the rest were used as test samples. After performance test of the trained neural network, the test results of Fy direction are shown in Figure 4 and 5, and similar in other directions. Decoupling precision of BP algorithm in six dimensions is listed in Table 2. The maximum of coupling error of type Ⅰ and Ⅱ is 0.5% and 2.9%, respectively. The results show that BP algorithm is superior to the decoupling algorithm mentioned in the previous section. Of course, the decoupling process time of this method is longer , reaching 3 seconds or so.

3.3. An optimized BP neural network based on GA

Many people found that the BP algorithm is very sensitive to the initial weights, and the neural network with different generalization performance will be obtained under the only condition that the initial weights are different. Using GA to optimize the initial weights of the neural network can find nearly optimal network connection weights without computing gradient information. Thus, GA is proposed to ameliorate the defect of BP algorithm that is easy to fall into local minimum in this paper.

The basic steps of the optimized BP neural network by GA are as follows:

Step 1 Determine BP neural network topology, and construct this network.

Step 2 Initialize relevant operating parameters of the GA: population size, crossover probability, mutation probability, etc.

Step 3 Create an initial population, and use formula (4) to encode every individual.

Step 4 Calculate the fitness of each individual. Select the inverse of the test error of BP neural network as individual fitness. The flow chart of fitness calculation is as shown in Figure 6.

Step 5 Population evolutions. Population evolutions include selection, crossover and mutation.

Step 6 Determine weather to achieve optimal target. If yes, terminate optimization process of GA; otherwise, turn to step 4.

The best individual in the last population can be used as the approximate optimal solution, i.e. optimal initial weights and biases of BP network. Overall schematic representation of optimized GA-BP neural network is shown in Figure 8.

Table 3. The number of weights and biases in decoupling neural network.

Weights between input layer and hidden layer	Biases of hidden layer	Weights between hidden layer and output layer	Biases of output layer	total
60	10	60	6	136

Table 4. Operating parameters of GA.

Population size	Maximum number of genetic generations	Crossover probability	Mutation probability
40	20	0.6	0.1

3.3.1 Determine encoding mode and encoding length. GA starts from a population with potential solution sets. The population is comprised of a certain number of encoded gene individuals. One of the key issues of constructing genetic algorithm is the encoding method of chromosome. Real number encoding method is adopted in the decoupling model of six-axis force/torque sensor. The complete coding strand of a chromosome is composed of connection weights between input layer and hidden layer, bias of hidden layer, connection weights between hidden layer and output layer, and bias of output layer. The encoding length of individuals is expressed as follows:

$$L = inputnum \times hiddennum + hiddennum + hiddennum \times outputnum + outputnum \quad (3)$$

where L is the coding length of individuals; $inputnum$, $hiddennum$, and $outputnum$ is the number of neurons of input layer, hidden layer and output layer of BP network, respectively.

In view of the architecture of this decoupling neural network, the number of weights and bias is shown in Table 3, and thus the total coding length of chromosome is 136.

3.3.2 Initialize the population. The chromosome of population is encoded as

$$w_{11}^{(1)}w_{12}^{(1)}\cdots w_{1,10}^{(1)}w_{21}^{(1)}w_{22}^{(1)}\cdots w_{2,10}^{(1)}w_{31}^{(1)}\cdots w_{6,10}^{(1)}b_1b_2\cdots b_{10}w_{11}^{(2)}w_{12}^{(2)}\cdots w_{16}^{(2)}w_{21}^{(2)}\cdots w_{10,6}^{(2)}c_1c_2\cdots c_6 \quad (4)$$

where $w_{ij}^{(1)}$, $w_{kl}^{(2)}$ is connection weight from the i^{th} input neuron to the j^{th} hidden neuron and weight from the k^{th} hidden neuron to the l^{th} output neuron, respectively, and b_m, c_n represents threshold of the m^{th} hidden neuron and the n^{th} output neuron, respectively.
Initialize basic parameters of the GA: population size is 40, crossover probability is 0.6, mutation probability is 0.1, maximum number of genetic generations is 20. Operating parameters of GA are initialized as showed in Table 4.

3.3.3 Fitness function. The initial weights and thresholds of BP neural network are obtained by decoding individual. Calculate sum of absolute value of errors between the predicted output and the desired output of the BP network， and then calculate it's reciprocal to be acted as the individual's fitness. The correlation formula is shown as follow:

$$F=\left(\sum_{i=1}^{n}abs(y_i-o_i)\right)^{-1} \quad (5)$$

Here, F is the individual's fitness; n is the number of the output layer neurons of the neural network; y_i and o_i is the expected and predicted output of the i^{th} output neuron, respectively.

3.3.4 Population evolutions. In each generation, individuals are selected according to individual fitness values. With the help of genetic operators, a population representing a new set of solution are produced by crossover and mutation. The roulette wheel is used in selection operation. The basic idea of this method is the probability of individual selection is proportional to the fitness function. The flow chart of population evolutions are shown as Figure 7.

3.3.5 Decoupling results analysis. The fitness evolution curve of the optimized BP decoupling network based on GA is shown as Figure 9. It can be seen from the figure that the prediction error decreases gradually with the evolution, and when the evolution to the 10 generation, the trend of decline is slow. Figure 10 shows the prediction error comparison between BP and GA-BP network. It is easy to see that GA-BP network is better than BP network by comparison of training results.

Table 5. Decoupling precision of optimized BP network by GA in six dimensions.

Coupling error(FS%)	Fx	Fy	Fz	Mx	My	Mz
Type Ⅰ	0.18	0.14	0.21	0.3	0.35	0.1
Type Ⅱ	2.1	1.9	2.2	1.0	2.3	1.3

As can be seen from Table 5, the maximum of coupling error of type Ⅰ and type Ⅱ is 0.35% and 2.3%, respectively. The results show that the proposed decoupling algorithm in this section is superior to BP algorithm in decoupling precision. Althouth this decoupling algorithm has the highest accuracy of the three methods mentioned above, the decoupling time is the longest. It takes about 5 minites to complete a decoupling process and not suitable for online decoupling.

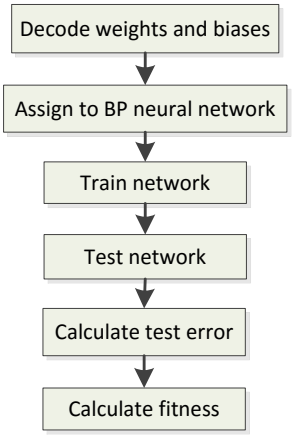

Figure 6. Flow chart of fitness calculation.

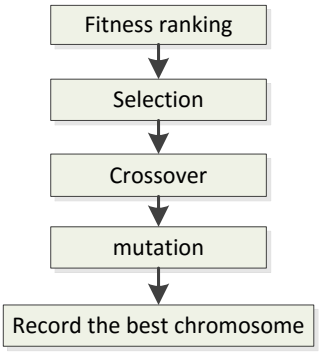

Figure 7. Flow chart of population evolutions.

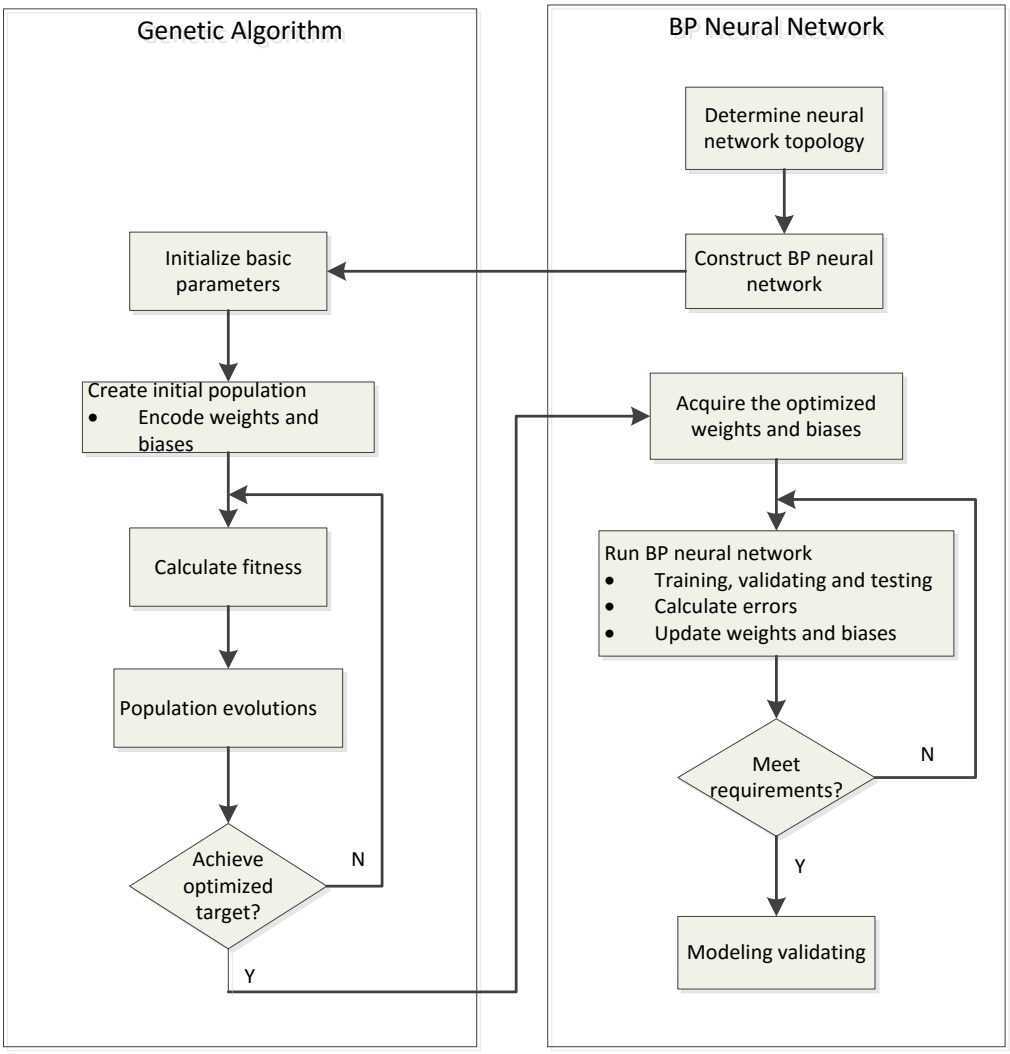

Figure 8. Flow chart of GA-BP algorithm.

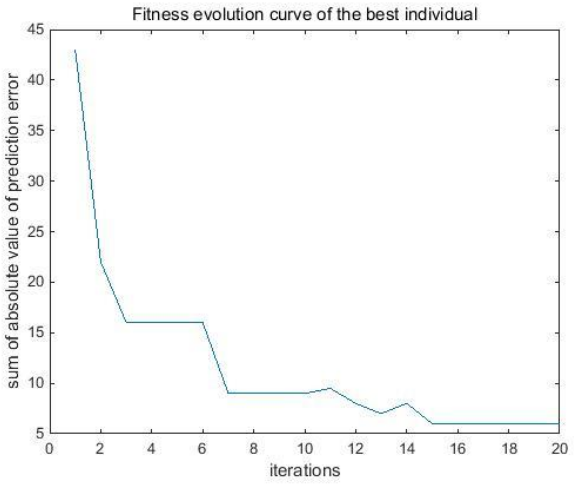

Figure 9. The fitness evolution curve.

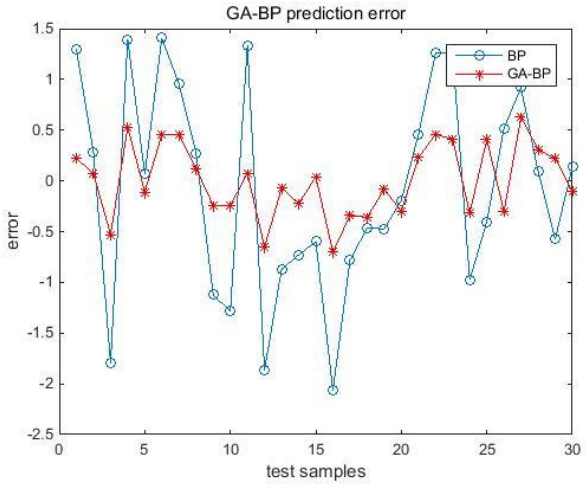

Figure 10. Prediction error comparison between BP and GA-BP network.

4. Conclusion

In the light of the low decoupling accuracy of traditional decoupling algorithms, GA-BP algorithm used for static decoupling of 6-axis force/torque sensor is proposed in this paper. GA is used to optimize the initial weights and biases of the BP neural network. Besides, decoupling algorithm based on calculating the pseudo-inverse matrix of calibration and classical BP algorithm are selected for comparison in order to verify the validity of the proposed algorithm. The maximum coupling error type of Ⅰ is 0.83%, 0.51%, 0.35%, respectively, and the maximum coupling error type of Ⅱ is 8.7%, 2.9%, 2.3%, respectively. The decoupling analysis results indicate that GA-BP decoupling algorithm has the highest accuracy of the three algorithms mentioned in this paper, the decoupling time, however, is the longest. It is appropriate for accurate decoupling offline.

5. Appendices

type Ⅰ: It reflects the degree of deviation between the measured value and the actual applied value of a certain dimension.

type Ⅱ: It reflects the interference size in the direction of *i*, while a force/moment not applied in this direction, whereas applied in other directions.

$$\text{type I}=\left|\frac{e_{i(\max)}}{Y_{i(F.S)}}\right|, \quad i=1,2,\cdots\cdots,6 \tag{A.1}$$

$$\text{type II}=\sqrt{\frac{\sum\left|y_{ij(\max)}\right|^2}{\left|Y_{i(F.S)}\right|^2}}, j=1,2,\cdots\cdots,6, i\neq j \tag{A.2}$$

where $e_{i(\max)}$ is the difference between the measured value and the actual applied value in the direction of i, $Y_{i(F.S)}$ represents the full scale value of the force/torque that can be applied in the direction of i, and $y_{ij(\max)}$ represents the maximum force/torque value measured in the direction of i when the force/torque is applied in the direction of j and not in the other five directions.

6. References

[1] Song Aiguo, Wu Juan, Qin Gang and Huang Weiyi 2007 A novel self-decoupled four degree-of-freedom wrist force/torque sensor *Meas*. **40** 883–91
[2] Wu Bo and Cai Ping 2013 Decoupling analysis of a sliding structure six-axis force/torque sensor *Meas. Sci. Rev.* **13** 187–93
[3] Beyeler F, Muntwyler S *et al* 2009 *IEEE Int. Conf. on Robotics and Automation (Kobe)* pp 520–525
[4] Cao Huibin, Sun Yuxiang, Liu Limin, Feng Yong, Wang Yijun and Ge Yunjian 2011 Coupling analysis of multi-axis force sensor and research of decoupling method *Chinese Journal of Sensors and Actuators* **24** 1136–40
[5] Jiang Li, Liu Hong and Cai Hegao 2004 Nonlinear static decoupling of multi-axis force/torque sensor *Chinese Journal of Scientific Instrument* **25** 284–7
[6] Chen Danfeng, Song Aiguo and Li Ang 2015 Design and calibration of a six-axis force/torque sensor with large measurement range used for the space manipulator. *Proc. Eng.* **99** 1164–70
[7] Yao X 1999 Evolving artificial neural networks. *Proc. IEEE* **87** 1423–47
[8] Venkadesh S and Hoogenboom G 2013 A genetic algorithm to refine input data selection for air temperature prediction using artificial neural networks. *Appl. Soft Comput.* **13** 2253–60
[9] Maarouf M, Sosa A *et al* 2015 The role of artificial neural networks in evolutionary optimization: a review *Computational Methods in Applied Sciences* (Switzerland: Springer) chapter 4 pp 59–76
[10] Sun Wei and Xu Yanfeng 2016 Financial security Evaluation of the electric power industry in china based on a back propagation neural network optimized by genetic algorithm *Energy* **101** 366–79
[11] Sharon Mano J Pappu and Sathyanarayana N G 2017 Artificial neural network and regression coupled genetic algorithm to optimize parameters for enhanced xylitol production by debaryomyces nepalensis in bioreactor *Biochem. Eng. J.* **120** 136–145
[12] Jia Weikuan, Zhao Dean and Ding Ling 2016 An optimized RBF neural network algorithm based on partial least squares and genetic algorithm for classification of small sample. *Appl. Soft Comput.* **48** 373–384